Earth and Planetary Science Letters 391 (2014) 16–23

Contents lists available at ScienceDirect

Earth and Planetary Science Letters

www.elsevier.com/locate/epsl

Abrupt weakening of the Indian summer monsoon at 8.2 kyr B.P.

Yama Dixit [a,*], David A. Hodell [a], Rajiv Sinha [b], Cameron A. Petrie [c]

[a] Godwin Laboratory for Palaeoclimate Research, Department of Earth Sciences, University of Cambridge, Cambridge, CB2 3EQ, United Kingdom
[b] Department of Civil Engineering, Indian Institute of Technology, Kanpur, India
[c] Department of Archaeology and Anthropology, University of Cambridge, United Kingdom

ARTICLE INFO

Article history:
Received 19 June 2013
Received in revised form 17 December 2013
Accepted 20 January 2014
Available online 7 February 2014
Editor: J. Lynch-Stieglitz

Keywords:
paleoclimate
stable isotopes

ABSTRACT

An oxygen isotope record of biogenic carbonate from paleolake Riwasa in northwestern (NW) India provides a history of the Indian Summer Monsoon (ISM) from ~11 to 6 kyr B.P. The lake was dry throughout the Late Glacial period when aeolian sands were deposited. Lacustrine sedimentation commenced in the early Holocene and the lake deepened significantly at ~9.4 kyr B.P., indicating a strengthening of the ISM in response to summer insolation forcing. This high lake stand was interrupted by an abrupt desiccation, which is marked by a 12-cm limestone hardground that formed during a period of sub-aerial exposure after ~8.3 kyr B.P. The base of the hardground surface coincides with the beginning of the '8.2-kyr B.P. cooling event' in the North Atlantic that has been associated with a glacial outburst flood and slowdown of Atlantic meridional overturning circulation. The hardground provides robust evidence of a weakening of the ISM on the Indian subcontinent at ~8.2 kyr B.P., and supports previous results of a strong teleconnection between monsoon Asia and North Atlantic climate. Lacustrine sedimentation resumed at ~7.9 kyr B.P. suggesting the 8.2-kyr desiccation of paleolake Riwasa represented an abrupt response of the ISM to forcing from the North Atlantic.

1. Introduction

Changes in the intensity of the Indian Summer Monsoon (ISM) have been inferred from marine sediments in the Arabian Sea (Overpeck et al., 1996; Schulz et al., 1998; Sarkar et al., 2000; Staubwasser et al., 2003; Gupta et al., 2005; Govil and Naidu, 2010), Bay of Bengal (Rashid et al., 2011; Govil et al., 2011), Andaman Sea (Rashid et al., 2007) and speleothems from Oman and China (Neff et al., 2001; Fleitmann et al., 2007; Wang et al., 2005; Cai et al., 2012; Liu et al., 2013). Relatively few Holocene terrestrial palaeoclimate records exist, however, from the Indian subcontinent (Prasad and Enzel, 2006; Sinha et al., 2006; Berkelhammer et al., 2012).

Most records in NW India are from playa lake deposits in the Thar Desert (Prasad and Enzel, 2006 and references therein; Sinha et al., 2006). The climate histories of these lakes do not match the evolution of the ISM as inferred from marine and speleothem records (Prasad and Enzel, 2006). The latter archives indicate that monsoon intensity responded to orbitally-forced changes in summer insolation by increasing to a maximum in the early Holocene and gradually declining after ~7 kyr B.P. (Overpeck et al., 1996; Wang et al., 2005; Cai et al., 2012). In contrast, the Thar Desert lakes appeared in the wake of increasing summer monsoon in the early Holocene, but the maximum levels of Lakes Lunkaransar and Didwana occurred between ~7 and 5.3 kyr B.P. during the middle Holocene and Sambhar Lake does not show any evidence of complete desiccation throughout its history (Sinha et al., 2006). The centennial-scale monsoon fluctuations inferred from marine and speleothem records are also not recorded in the paleolimnological history of the Thar lakes. The divergent climate history of the Thar lakes has been attributed to changing winter precipitation in the mid-Holocene that evolved independently of changing strength of the ISM (Enzel et al., 1999).

Here we reconstruct the history of ISM variability on the Indian subcontinent during the early-middle Holocene using a sedimentary record from a paleolake at Riwasa, Haryana State, which is located ~140 km west of Delhi in the semi-arid zone on the NE margin of the Thar Desert (Fig. 1). The paleolake existed in a region where the annual rainfall gradient is steep (varying between 200 and 600 mm in 150 km). The hydrology of this closed-basin lake was sensitive to past changes in monsoon rainfall and evaporation, which is recorded by the oxygen isotope ratio of carbonate shells of ostracods and gastropods preserved in lake sediment. We found the intensity of the ISM generally responded to long-term orbital forcing through the Holocene, but also exhibited an abrupt response at 8.2 kyr B.P. with a strong teleconnection to North Atlantic climate.

* Corresponding author. Tel.: +44 (0) 1223 333441.
E-mail address: yd234@cam.ac.uk (Y. Dixit).

http://dx.doi.org/10.1016/j.epsl.2014.01.026

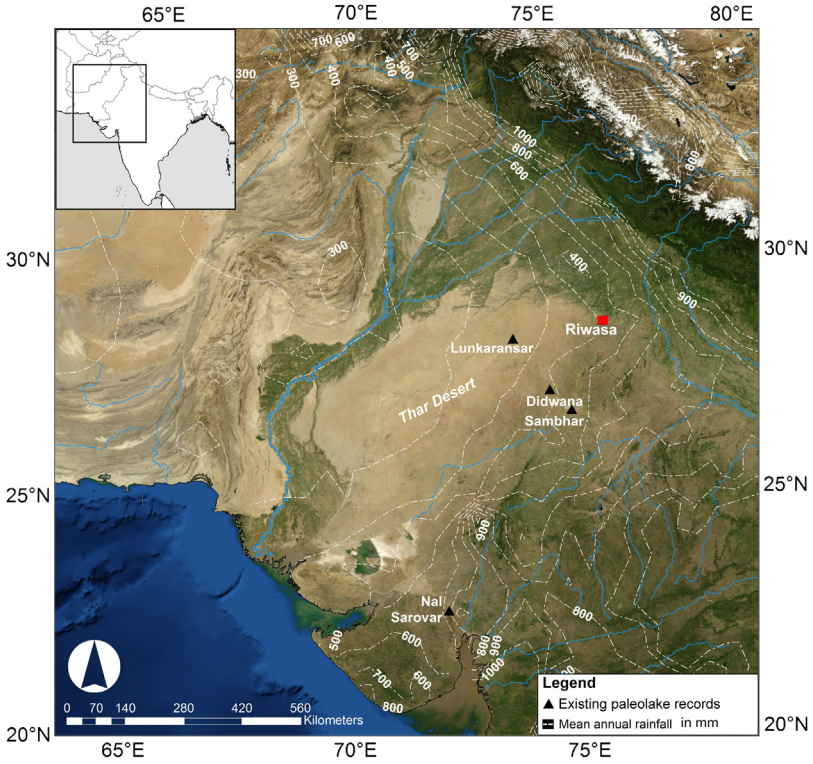

Fig. 1. Map of Northwest India showing the location of previously published lake records (black triangles) and paleolake Riwasa (red square), Haryana. Inset shows the Indian Subcontinent in South Asia. The white dotted lines are 100 mm isohyets for areas receiving between 0 and 1000 mm mean annual rainfall (in mm) for the period between 1900–2008. NASA Blue Marble: Next Generation satellite imagery was obtained from NASA's Earth Observatory. (For interpretation of the references to color in this figure legend, the reader is referred to the web version of this article.)

2. Regional setting

Samples of paleolake Riwasa sediment were obtained from a well section (N 28°47′21.6″, E 075°57′24.6″) located ∼1 km south of Riwasa village in the Bhiwani District in Haryana state, India. The Riwasa lacustrine deposits were once part of a large lake system that occupied low-lying areas (Saini et al., 2005). The lake deposits are scattered as small lenses of sediment composed of shelly silt-clay that are interrupted by aeolian sand dunes and inselbergs composed of granite and rhyolite (Fig. S1). The thickness of lacustrine sediment varies from 0.4 to 2.5 m in the region (Saini et al., 2005).

A climate record spanning the past 85 yr from a nearby meteorological station in Hissar, located 70 km northwest of Riwasa, indicates a mean annual temperature of 25.2 °C with maximum temperatures in June (41.1 °C) and minimum temperatures in January (5 °C) (Indian Meteorological Department, 2000). Relative humidity ranges from 24 to 75% annually. The Riwasa area receives annual rainfall of 300–500 mm, about 80% of which falls under the influence of the Bay of Bengal arm of the strong southwesterly summer monsoon between the months of June and September (Bhattacharya et al., 2003; Sengupta and Sarkar, 2006). The remaining winter rainfall comes during the months of November to March when N-NW winds bring relatively dry air to NW India. The potential evapotranspiration is 40 mm in December and 222.3 mm in June and the average annual evapotranspiration ranges from 160–200 mm (Indian Meteorological Department, 2000). Paleolake Riwasa was a closed basin in the Holocene. Hydrological inputs to the lake included precipitation falling directly on the lake, runoff, and subsurface seepage. Hydrologic losses are mainly through evaporation, which is seasonally very high under semi-arid climate conditions.

3. Materials and methods

We sampled a 2.8-m section from an exposed well to the south of the village of Riwasa. Depths in section are relative to the well surface. The uppermost 30-cm of sediments were disregarded owing to disturbance by modern cultivation. Below this level, the sediment section was sampled every 2 cm down to 1.08 m. Sediments below 1.08 m are underlain by a well-lithified hardground, which is 12-cm thick at the well section. The hardground was sampled with a hammer and chisel because of its well-indurated nature. Sediment samples below the hardground were taken every 2-cm to a level of ∼2.8 m at the bottom of the well.

Bulk sediments were crushed and dried at 60 °C for carbonate analysis. Weight percent $CaCO_3$ was determined by coulometric titration (Engleman et al., 1985). Analytical precision was estimated by analysis of 94 reagent-grade $CaCO_3$ (100%) standards that yielded a mean and standard deviation (1σ) of $99.97 \pm 0.82\%$.

Paleolake Riwasa sediments contain well-preserved ostracods and gastropods. Calcite carapaces of *Cyprideis torosa* and aragonite shells of *Melanoides tuberculata* were used for oxygen isotope analysis. Both male and female specimens of adult *C. torosa* secrete their shells at near oxygen isotopic equilibrium with the lake water (Durazzi, 1977; Marco-Barba et al., 2012). *C. torosa* (Fig. S2) is part of the meiobenthos and lives in shallow brackish environments where large amounts of organic detritus are present. The species is euryhaline and tolerant of salinities up to 60‰ (Heip, 1976), and generally associated with lake water chemistry dominated by Na and Cl ions. *C. torosa* undergoes one molt generation annually (Herman et al., 1983; Marco-Barba et al., 2012) and requires permanent water to reproduce because its eggs cannot withstand desiccation (Anadon et al., 1986). The shells of *C. torosa* can display nodings or ornamentation at lower salinities and have smooth

Table 1
Riwasa radiocarbon analyses, calibrated using OxCal v.4.1.63 and the IntCal09 data set (Reimer et al., 2009). Sediment depths were converted to age with an equation derived by interpolation between 5 depth-age points. The date denoted by * has been rejected due to poor preservation of the shell fragments (Fig. S3).

Depth (cm)	Lab No. (CAMS#)	Material	Radiocarbon age ^{14}C (yr B.P.)	Calibrated age (2σ) (yr B.P.)
70	150823	Gastropods	6270 ± 45	7021–7289
96	150824	Gastropods	6835 ± 30	7607–7725
121	147510	Ostracods	7505 ± 45	8200–8396
155	147511	Ostracods	7945 ± 40	8643–8982
186	150825	Gastropods	8480 ± 35	9453–9535
247–278*	152730	Gastropods	8665 ± 40	9539–9702

carapace surface at higher salinities (above 10‰) (Carbonel et al., 1988). In Riwasa sediments, *C. torosa* shells are smooth indicative of salinities exceeding 10‰.

M. tuberculata (Fig. S3) is a prosobranch (gill breathing) gastropod, occurring abundantly in a range of fresh-to-brackish water habitats. *M. tuberculata* secretes its aragonitic shell in near oxygen isotopic equilibrium with lake water (Shanahan et al., 2005) and grows throughout a life span of 1 to 5 yr. Isotopic analysis of this species has proven useful for paleoclimate reconstruction (Leng et al., 1999). Whereas an inter-seasonal climate signal can be obtained by serially sampling gastropods along the growth axis, we conducted isotope analysis on whole shells that integrate seasonal changes over a period of up to 5 yr (Leng et al., 1999).

Samples for stable isotope analysis were wet sieved (at 63 microns) and the coarse fraction was collected and dried overnight at 50 °C. About 10–20 well-preserved carapaces (weighing more than 300 µg) of the ostracod *C. torosa* and between 2–5 adult gastropod shells were selected from the sieved 300–500 µm fraction in each sample under a binocular microscope at 10× magnification. Ostracod and gastropod shells were gently crushed, sonicated in methanol, and rinsed in double-distilled water to remove fine-grained clay particles. Crushed samples were dried overnight and loaded into the vials for analysis using a Multicarb preparation system coupled to a VG SIRA Mass Spectrometer in the Godwin Laboratory at the University of Cambridge.

Bulk sediment samples were ground to a fine powder and stable isotopes of carbonate were measured using a ThermoScientific GasBench II, equipped with a CTC autosampler coupled to a MAT253 mass spectrometer. Analytical precision for δ^{18}O was estimated at ±0.1‰ by repeated analysis of the Carrara Marble standard. Results are reported relative to the Vienna Pee Dee Belemnite (VPDB).

The chronology of the Riwasa well section was determined by radiocarbon dating of ostracod and gastropod shells by Accelerator Mass Spectrometry (AMS) at the Center for AMS (CAMS), Lawrence Livermore National Laboratory, USA. Typically about 15–20 ostracods and 1–2 gastropod specimens were crushed, cleaned with methanol and deionized water, weighed, and submitted for radiocarbon analysis. Prior to target preparation at CAMS, shells were gently leached in dilute hydrochloric acid (1N) to remove the surface layer that is susceptible to diagenetic alteration. The lack of co-occurring shells and datable organic material from the Riwasa sediment section hindered estimation of reservoir age. Because bedrock in the region is composed mainly of igneous rocks exposed as inselbergs (Chopra, 1990), the contribution of dead carbon from the catchment is assumed to be small (see Supplementary materials for detailed discussion). In addition, the large surface area to volume of this shallow lake system should promote CO_2 equilibration with the atmosphere (Broecker and Walton, 1959). Radiocarbon dates were calibrated using OxCal v.4.1.63 and the IntCal09 data set (Reimer et al., 2009). Calibrated ages are expressed as kiloyears before present (kyr B.P.).

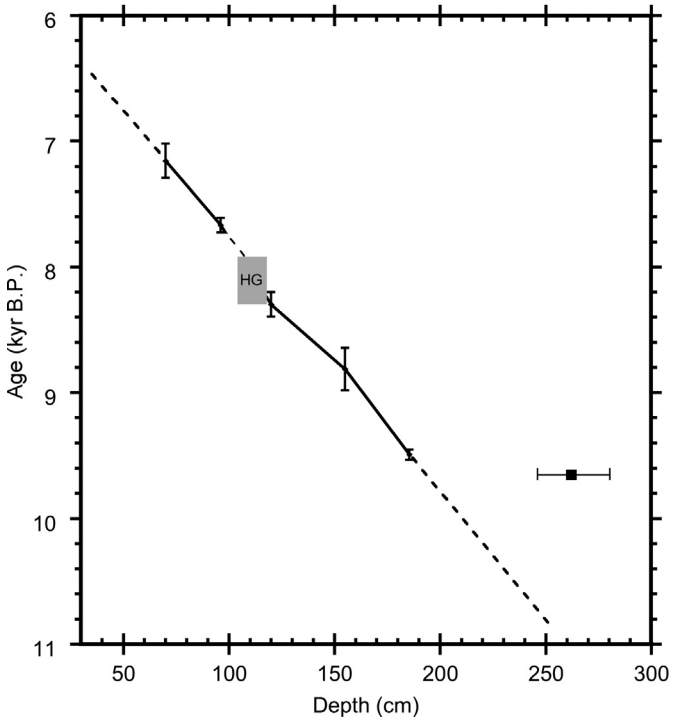

Fig. 2. Depth versus age plot for the Riwasa section. Radiocarbon dates were converted to calendar years with the program calibrated using OxCal v.4.1.63 and the IntCal09 data set (Reimer et al., 2009). Calibrated age is reported over 2σ error range. Sediment depths were converted to age using equations derived by interpolation of depth-age points from 70 to 96 cm, 121 to 155 cm and 155 to 186 cm. Black square represents the age obtained on shell fragments from 247–278 cm that were combined over a 31 cm interval for radiocarbon dating because of insufficient material. The shell fragments yielded a younger age because of diagenetic alteration and precipitation of secondary calcite on the aragonite shells. The date was rejected due to poor preservation of the shell fragments (Fig. S4). The age of the top and base of the section is calculated by extrapolation of the regression lines (dashed lines).

4. Results

4.1. Chronology

The five age-depth pairs in the Riwasa section are ordered sequentially. Sediment depths were converted to age by assuming linear sedimentation rates between depth-age points; i.e., between 70 and 96 cm, 121 and 155 cm, 155 and 186 cm (Table 1, Fig. 2). The age for the top of the section was estimated by extrapolating the sedimentation rate (51 cm kyr^{-1}) between 70 and 96 cm to the surface. The sedimentation rate was highest (68 cm kyr^{-1}) between 121 and 155 cm, during the period from 8.8 to 8.3 kyr B.P. Owing to the paucity of whole shells in sediment horizons near the base of the section, we dated shell fragments of gastropods combined from depths between 247 and 278 cm. The resulting date yielded very high sedimentation rates (612 cm kyr^{-1}) for the lower part of the section. Subsequent XRD analysis showed the gastropod

shell fragments, which were originally aragonite, had been diagenetically altered to calcite (Fig. S4). We therefore rejected the lowermost date and estimated ages below 9.4 kyr B.P. by extrapolating the sedimentation rate (44.8 cm kyr^{-1}) of the overlying interval (155 to 186 cm) to the base of the section (Fig. 2).

Because gastropods and ostracods are heavily cemented in the hardground, we bracketed the age of the hardground (108–120 cm) by dating the nearest horizon above and below it that contained sufficiently well preserved shells for radiocarbon analysis (see Supplementary materials for detailed discussion). The age of the base of the hardground is ~8.3 kyr B.P. (8.2 to ~8.4 kyr B.P.) on the basis of a radiocarbon date of ostracods at 121 cm. The formation of the hardground was, therefore, younger than 8.3 kyr B.P. The closest date obtained above the hardground surface was ~7.7 kyr B.P. at 96 cm (Table 1). Owing to a paucity of sufficiently well-preserved material for radiocarbon dating from just above the hardground at 108 cm and considering that the sediment lithology following the hardground is same to the top of the section, we estimated the age of the resumption of lake sedimentation following the hardground by extrapolating the sedimentation rate (51 cm kyr^{-1}) from the interval above (70 to 96 cm). The age for the end of the hardground formation at 108 cm is 7.9 ± 0.1 kyr B.P.

4.2. Lithology

The Riwasa section was first described by Saini et al. (2005) and assumed to be Holocene although no radiocarbon dates were available. The sediment sequence is divided into five principal lithologic units. Lowermost Unit V (3.57 to 2.54 m) is light-brown, fine-grained, and well-sorted sand that is interpreted as an aeolian deposit. After ~11 kyr B.P. (at 2.54 m), the aeolian sand grades into shell-bearing, lacustrine Unit IV with ~27% $CaCO_3$ content (Fig. 3). Unit IV is subdivided into two subunits on the basis of color, grain size, and the first occurrence of gastropods. Unit IVa consists of grayish shelly coarse silt to very fine sand (2.54 to 2.28 m) and grades into Unit IVb (2.28 to 1.8 m) composed of greenish silt containing gastropods and ostracods (Fig. S8). Unit IV is overlain by the main lake Unit III deposited between ~9.4 and 8.3 kyr B.P (1.80 to 1.21 m). It consists of unconsolidated, shell-bearing clay grading into white, shell-bearing, massive calcareous mud with carbonate content averaging ~65%.

Unit III is capped by a 12-cm-thick argillaceous shelly limestone 'hardground' (Unit II) that has a 4-cm, dark gray calcite-cemented upper surface with high carbonate content (up to ~80%). The cement is composed of calcite with minor traces of quartz and halite (Fig. S7). Texturally, the hardground is composed of limestone containing whole shells and fragments of gastropods and ostracods (Figs. S5, S6). The hardground contains fossil roots and rootlets (Fig. S5) and an abundance of well-preserved boring gastropod fauna. Beginning at 1.08 m (~7.9 kyr B.P.) and continuing to the top of the section, Unit I consists of silty sand with fewer shells and decreased carbonate content (~10%) (Fig. 3).

4.3. Oxygen isotopes

During the Last Glacial period before ~11 kyr B.P., aeolian sands were deposited that are devoid of aquatic shells. Between ~11 and 9.4 kyr B.P. (Unit III), oxygen isotopes of ostracods average 1‰. Gastropods first appear in the section at ~10.4 kyr B.P. with an average $\delta^{18}O$ value of ~0.8‰ between 10.4 and 9.4 kyr B.P., which is similar to the average ostracod $\delta^{18}O$ values for this period. The bulk carbonate $\delta^{18}O$ values have an average of −3.7‰ with a peak at ~9.6 kyr B.P. (Fig. S9). Both biogenic and bulk carbonate oxygen isotopes gradually decrease after ~9.4 kyr B.P. Ostracod $\delta^{18}O$ averages −1.3‰ and the gastropod $\delta^{18}O$ values average −3.2‰

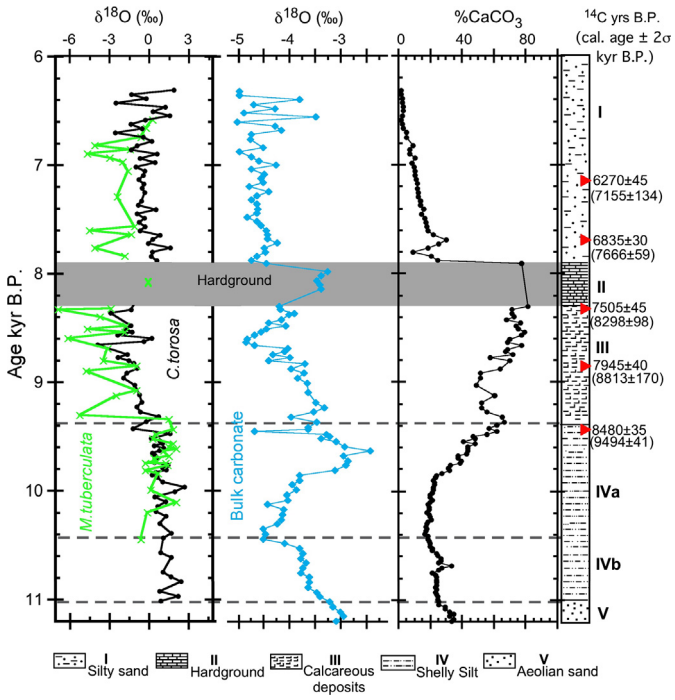

Fig. 3. Oxygen isotopes of the ostracod *Cyprideis torosa* (black), gastropod *Melanoides tuberculata* (green), bulk sediment carbonate $\delta^{18}O$ (blue), and weight percent calcium carbonate from paleolake Riwasa sediments versus calibrated age in kiloyear B.P. Green cross in the hardground is the average $\delta^{18}O$ of the *M. tuberculata* fragments broken off from the exposed shell cemented in the hardground. To the right is a lithologic log of the section (Unit I–V) with red triangles denoting the levels of AMS radiocarbon dates. Horizontal grey bar denote the hardground after ~8.3 kyr B.P. Black dashed lines denote the major hydrological changes in the Riwasa section. (For interpretation of the references to color in this figure legend, the reader is referred to the web version of this article.)

between ~9.4 and 8.3 kyr B.P. (Unit II). The gastropod oxygen isotopes in the section are more variable compared to the ostracod signal because each data point for gastropod $\delta^{18}O$ was obtained on powder by crushing 1–2 gastropod specimens. On the contrary, each sample for ostracod $\delta^{18}O$ was measured on 15–20 crushed carapaces, which yields the mean value of the lifespans of each individual. Moreover, gastropods are littoral organisms that record surface water temperatures that vary more so than bottom temperatures recorded by benthic ostracods.

Although biogenic carbonate is cemented in the hardground, it was possible to sample a few well-preserved gastropod shells by drilling, which yielded an average $\delta^{18}O$ value of −1.06‰. The $\delta^{18}O$ values of bulk carbonates increase by ~1‰ in the hardground layer (Fig. 3). The average $\delta^{18}O$ values for ostracod and gastropod in Unit I above the hardground are greater than those below, averaging −0.2‰ and −1.8‰, respectively.

5. Discussion

5.1. Interpretation of isotope variations

The $\delta^{18}O$ of biogenic carbonate is influenced by both temperature and the $\delta^{18}O$ of lake water. Because Riwasa was a closed basin during the Holocene, the $\delta^{18}O$ of lake water reflects the $\delta^{18}O$ of rainfall and the ratio of evaporation to precipitation (E/P) over the lake and its surrounding catchment. We assume changes in $\delta^{18}O$ related to temperature were small compared to those resulting from changing $\delta^{18}O$ of lake water because the temperature dependence of equilibrium isotope fractionation between calcite and water is ~−0.24‰/°C (Craig and Gordon, 1965).

Riwasa today receives 80% of its total rainfall during the summer monsoon season. The seasonal range in $\delta^{18}O$ of rainfall is very large at New Delhi, averaging $\sim -7.5‰$ during the summer monsoon season and $\sim 0.3‰$ during the dry season (Rozanski et al., 1993; Bhattacharya et al., 2003) (Fig. S10). Variation in the timing and intensity of the monsoon affects lake-water $\delta^{18}O$ by changing the $\delta^{18}O$ of rainfall and by altering the relative hydrologic balance between evaporation and precipitation in the lake catchment (Fasullo and Webster, 2003; Berkelhammer et al., 2012). An early monsoon withdrawal and/or a decrease in rainfall amount increases the annually mean weighted $\delta^{18}O$ of rainfall. Because the mean isotopic value of the Riwasa lake water reflects primarily the isotopic composition of the lighter summer rainfall averaged over time, we interpret increases in shell $\delta^{18}O$ to reflect a decreased contribution of summer monsoon rainfall and increased evaporation over the lake and its catchment. Conversely, wet periods of increased monsoonal rainfall and decreased evaporation are marked by lower shell $\delta^{18}O$.

The bulk carbonate in Riwasa sediments is comprised of biogenic carbonate (consisting of ostracod, gastropod shells and other skeletal carbonates), bio-induced authigenic carbonate, and secondary carbonate. Bio-induced authigenic calcite precipitation is favored by warm temperature and high rates of primary productivity that decrease the dissolved $^{12}CO_2$ and increases the pH, thereby shifting the carbonate equilibria towards greater carbonate ion concentration (Leng and Marshall, 2004; Hodell et al., 1998). Carbonate precipitation occurs during the summer-stratified period when lake temperature reaches a maximum and $\delta^{18}O$ of lake water is low owing to ^{18}O-depleted monsoon rainfall. Consequently, the $\delta^{18}O$ of bulk carbonate is considerably lower than co-occurring gastropods and ostracods. Low $\delta^{18}O$ and high $\delta^{13}C$ of bulk carbonate is a characteristic feature of bio-induced authigenic calcite precipitation in hydrologically closed lakes (Talbot, 1990).

5.2. Early Holocene (11–8.2 kyr B.P.)

During the Late Glacial period older than ~11 kyr B.P., sediments were composed of aeolian sands with no aquatic shells suggesting that the summer monsoon was too weak to support permanent water in the basin. The lake basin began to fill at ~11 kyr B.P., which is marked by the appearance of ostracods and a lithologic change from aeolian sand to shell-bearing silt. The transition from Unit V to IV reflects the establishment of the lake related to ISM strengthening in the early Holocene. The filling of Lake Riwasa at ~11 kyr B.P. is consistent with pollen profiles and geochemical results from Rajasthani lakes, which also indicate the development of several bodies of water in the Thar Desert during the early Holocene between 12 and 11 kyr B.P. (Prasad and Enzel, 2006).

After ~9.4 kyr B.P., the $\delta^{18}O$ of ostracod and gastropods decreased and sediment composition was dominated by $CaCO_3$ (Fig. S8). Bulk carbonate $\delta^{18}O$ decreased at ~9.4 kyr B.P. indicating increased monsoon rainfall and decreased E/P over the lake and surrounding catchment. This period marks the onset of the deep-water phase of Lake Riwasa.

Marine, lacustrine, and terrestrial records beyond the Indian subcontinent also support an intensification of the summer monsoon during the early Holocene. Sediment cores from the eastern and western Arabian Sea indicate strengthened summer monsoon in the early Holocene (Overpeck et al., 1996; Schulz et al., 1998; Anand et al., 2008). Because Chinese speleothems records also partly reflect changes in intensity of the Indian monsoon (Pausata et al., 2011), minimum $\delta^{18}O$ values in the stalagmites of Dongge Cave in China (Wang et al., 2005) and Tianmen Cave on the Tibetan Plateau (Cai et al., 2012) also support a strong ISM during the early Holocene. Likewise, low $\delta^{18}O$ values in speleothems from southern Oman (Fleitmann et al., 2003) and carbonates from Yunnan lakes (Hodell et al., 1999) have been interpreted as evidence of strong monsoons in the early Holocene. Zhang et al. (2011) reviewed lake and speleothem records from monsoon Asia and concluded that variations in the strength of the Indian and East Asian monsoon were synchronous during this period. In contrast, the interpretations of paleolimnological records from Thar Desert lakes do not support high lake levels during the early Holocene. The high evaporation rates (up to 1000 mm in western Rajasthan during summers) in the arid Thar Desert and lack of a large drainage basin contributed to lower lake levels and ephemeral conditions at paleolakes Lunkaransar and Didwana during the early Holocene (Prasad and Enzel, 2006).

Climate models and paleoclimate studies suggest that the early Holocene Indian monsoon intensification was forced externally by increased boreal summer insolation (Kutzbach and Street-Perott, 1985; Overpeck et al., 1996). The filling of the Riwasa basin after 11 kyr B.P. followed by lake deepening at 10.4 kyr B.P. is in response to the increasing boreal summer insolation during the early Holocene. Strengthening of the ISM during the early Holocene was also related to reduced Tibetan Plateau snow cover (Marzin and Braconnot, 2009). Marzin and Braconnot (2009) used a coupled ocean-atmosphere model to demonstrate that the second step in ISM enhancement at ~9.5 kyr B.P. could result from a seasonality of insolation in the Northern Hemisphere due to the precession variations and changes in snow cover over the Tibetan Plateau (Marzin and Braconnot, 2009). The model demonstrated that the celestial summer season was shorter at 9.5 kyr B.P. and the rainy season was longer than at present. Comparison of the Riwasa $\delta^{18}O$ record and the summer insolation at 30° N (Berger, 1978) suggests that the intensity of the ISM paralleled increased summer insolation after glacial climate boundary conditions (cold North Atlantic SST and Eurasian snow cover) were diminished during the early-mid Holocene.

5.3. The 8.2 kyr event

Although the Riwasa $\delta^{18}O$ record suggests a progressive strengthening of the summer monsoon from ~11 kyr B.P. onward, this trend was interrupted by an abrupt event after 8.3 kyr B.P. Just when Lake Riwasa was at its deepest between 9.4 and 8.3 kyr B.P., the lake dried out as evidenced by formation of a hardground in the sedimentary sequence (Fig. 3). The hardground represents a shoreline carbonate deposit formed by sub-aerial exposure and lithification of previously deposited calcareous lacustrine sediments. Plants that colonized the newly exposed lake bottom sediments left fossil root casts. The hardground is similar to the "beachrock hardground" described in marl lakes of southern Australia (Last, 1992; Chalaturnyk et al., 2005), except the cement is calcite at Riwasa rather than dolomite. Last (1992) suggested that both transformation (i.e. chemical and structural alteration of pre-existing minerals) and neo-formation (i.e. by precipitation directly from pore or lake fluids) processes can contribute to hardground formation in marl lakes. These two diagenetic processes altered the carbonate minerals and produced the hard, well-cemented Unit II encountered in the well section. A 1‰ increase in bulk carbonate $\delta^{18}O$ and ~2‰ increase in the average gastropod $\delta^{18}O$ in the hardground as compared to the preceding deep-water phase indicate higher E/P during this period. We suggest the hardground was related to an abrupt decline in summer monsoon precipitation that affected the plains of NW India after 8.3 kyr B.P.

The '8.2-kyr event' was the largest climatic excursion of the Holocene from the perspective of Greenland temperature change (Thomas et al., 2007, Alley and Ágústsdóttir, 2005). Greenland temperature dropped by 3 °C and methane declined by 80 ppbv, suggesting an important change in the hydrologic cycle (Kobashi

et al., 2007). Oxygen isotope evidence from radiometrically-dated speleothems point to a pronounced weakening of the Asian and Indian monsoons at 8.2 kyr B.P. that lasted approximately 100 to 150 yr (Cheng et al., 2009; Liu et al., 2013; Fleitmann et al., 2003; Morril et al., 2013).

The hardground in the Riwasa section provides evidence from the Indian subcontinent for the widespread nature of the weakening of the ISM after ~8.3 kyr B.P. The estimated age of hardground formation (i.e., from 8.2 ± 0.1 kyr to 7.9 ± 0.1 kyr B.P.) corresponds well with the timing of the 8.2-kyr event in Greenland (Kobashi et al., 2007). Weakening of the Indian and Asian monsoon at ~8.2 kyr B.P. has been linked previously to cooling of the North Atlantic (Wang et al., 2005; Gupta et al., 2003; Staubwasser et al., 2002; Cai et al., 2012) when temperatures fell by 3.3 ± 1.1 °C in less than 20 yr in Greenland (Kobashi et al., 2007). The cause of this prominent cooling has been linked to a glacial outburst flood of freshwater from Lake Agassiz thorough the Hudson Bay into the North Atlantic (Bauer and Ganopolski, 2004). Freshening of the North Atlantic may have resulted in diminished production of North Atlantic Deep Water (NADW) and a weakening of Atlantic Meridional Overturning Circulation (AMOC) (Barber et al., 1999; Kleiven et al., 2008). The resulting decrease in ocean heat transport caused a southward shift of the Inter-Tropical Convergence Zone (ITCZ) and weakening of monsoons in the northern hemisphere (Cheng et al., 2009). Coupled-climate model simulations suggest that the period of diminished NADW formation match quantitatively with the paleoclimate evidence for the '8.2 kyr event' (LeGrande et al., 2006). Apart from changes in the heat transport via ocean circulation, another possible mechanism proposed for the North Atlantic climate and monsoon teleconnection is via the atmosphere. A change in Eurasian ice cover reinforces the Northern hemisphere cooling and displaces the marine and terrestrial ITCZ, thereby weakening the monsoon (Liu et al., 2013).

In the last glacial period, fresh-water forcing of the North Atlantic during Heinrich Events were associated with weakening of the Indian and Asian monsoons (Sirocko et al., 1996; Schulz et al., 1998; Porter and An, 1995; Wang et al., 2001; Sinha et al., 2005). In contrast, the cooling and geographic extent of the ~8.2 kyr B.P. climate anomaly was much smaller than that produced by Heinrich events during the last glacial period (Jin et al., 2007). Nonetheless, it appears the ~8.2-kyr event had a significant weakening affect on the ISM (Fig. 4).

The lacustrine sedimentation at Riwasa resumed after the '8.2 kyr event', with relatively higher average $\delta^{18}O$ values for biogenic carbonate than recorded during the lacustrine highstand between 9.4 and 8.3 kyr B.P. The lack of covariance between oxygen and carbon isotopes of bulk carbonate after 8.3 kyr B.P. suggests that the bulk carbonate is mainly composed of secondary carbonate (Talbot, 1990) (Fig. S9). The progressive lowering of rainfall after the peak monsoon strength indicates that the ISM declined in response to the decreasing summer insolation during the mid Holocene. In contrast, the Rajasthani lakes were deepest during the mid-Holocene because the Thar Desert received increased winter precipitation during this period as is documented in the palynological studies (Singh et al., 1990). Increased precipitation and lower evaporation rates during the mid-Holocene winters in the Thar Desert, therefore, supported high lake levels from 7.5–5.3 kyr B.P.

6. Conclusions

Our results from paleolake Riwasa, NW India, suggest that the ISM responded to insolation forcing during the Holocene, reaching its greatest strength between 9.4 and 8.3 kyr B.P. when Lake Riwasa was at a highstand. Following this highstand period, Lake Riwasa abruptly desiccated between 8.3 and 7.9 kyr B.P. forming a 12-cm thick hardground. The hardground represents an abrupt weakening of the ISM, which coincided with the '8.2 kyr B.P.' cold event in the North Atlantic. The timing, abruptness, and severity of the desiccation event in NW India at 8.2 kyr B.P. suggest a direct impact of freshwater forcing in the North Atlantic on the ISM, providing the first terrestrial evidence of the 8.2 kyr drying from the Indian subcontinent.

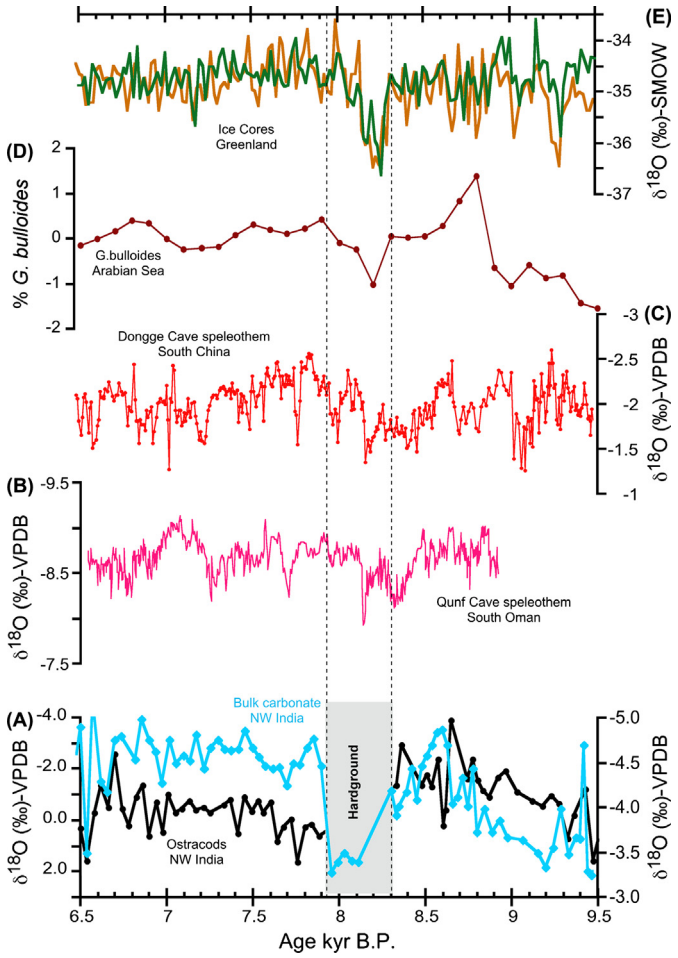

Fig. 4. Comparison of (A) $\delta^{18}O$ of ostracod calcite (black) and bulk carbonate (blue) record from Riwasa with (B) $\delta^{18}O$ of Qunf Cave speleothem in South Oman (Fleitmann et al., 2003), (C) $\delta^{18}O$ of Dongge Cave speleothem in China (Wang et al., 2005), (D) Abundance change in *G. bulloides* from the Arabian Sea (Gupta et al., 2003), (E) NGRIP (orange) and GRIP (green) $\delta^{18}O_{ice}$ (VSMOW) (Rasmussen et al., 2006). The grey bar represent 'hardground' at Riwasa and dashed lines ~7.9 to 8.3 kyr B.P. shows the approximate time of inferred decreased monsoon intensity from Oman, Arabian Sea and China, which is near coincident with the North Atlantic cooling event at ~8.2 kyr B.P. VPDB – Vienna Peedee Belemnite; VSMOW – Vienna Standard Mean Ocean Water. (For interpretation of the references to color in this figure legend, the reader is referred to the web version of this article.)

Acknowledgements

This work was supported by the Natural Environmental Research Council (NE/H011463/1). Yama Dixit has been funded by the Gates Cambridge Trust. We thank Mike Hall and James Rolfe for analytical assistance, Vikas Pawar and Ravindra Dixit for logistical field support, Thomas Guilderson for AMS radiocarbon dating measurements and David Redhouse for his assistance in processing the rainfall data and satellite imagery.

Appendix A. Supplementary material

Supplementary material related to this article can be found online at http://dx.doi.org/10.1016/j.epsl.2014.01.026.

References

Alley, R.B., Ágústsdóttir, A.M., 2005. The 8k event: cause and consequences of a major Holocene abrupt climate change. Quat. Sci. Rev. 24, 1123–1149.

Anadon, P., Dedeckker, P., Julia, R., 1986. The Pleistocene lake deposits of the NE Baza Basin (Spain) – salinity variations and ostracod succession. Hydrobiologia 143, 199–208.

Anand, P., Kroon, D., Singh, A.D., Ganeshram, R.S., Ganssen, G., Elderfield, H., 2008. Coupled sea surface temperature – seawater δ^{18}O reconstructions in the Arabian Sea at the millennial scale for the last 35 ka. Paleoceanography 23, PA4207. http://dx.doi.org/10.1029/2007PA001564.

Barber, D.C., Dyke, A., Hillaire-Marcel, C., Jennings, A.E., Andrews, J.T., Kerwin, M.W., Bilodeau, G., McNeely, R., Southon, J., Morehead, M.D., Gagnon, J.M., 1999. Forcing of the cold event of 8200 years ago by catastrophic drainage of Laurentide lakes. Nature 400, 344–348.

Bauer, E., Ganopolski, A., 2004. Simulation of the cold climate event 8200 years ago by meltwater outburst from Lake Agassiz. Paleoceanography 19, PA 3014.

Berkelhammer, M., Sinha, A., Stott, L., Cheng, H., Pausata, F.S.R., Yoshimura, K., 2012. An abrupt shift in the Indian monsoon 4000 years ago. Geophys. Monogr. 198, 75–87.

Berger, A., 1978. Long-term variations of daily insolation and Quaternary climatic change. J. Atmos. Sci. 35, 2362–2367.

Bhattacharya, S.K., Froehlich, K., Aggarwal, P.K., Kulkarni, K.M., 2003. Isotopic variation in Indian monsoon precipitation: Records from Bombay and New Delhi. Geophys. Res. Lett. 30, 2285. http://dx.doi.org/10.1029/2003GL018453.

Broecker, W.S., Walton, A., 1959. The geochemistry of C^{14} in fresh-water systems. Geochim. Cosmochim. Acta 16, 15–138.

Cai, Y., Zhang, H., Cheng, H., An, Z., Edwards, E., Wang, X., Tan, L., Liang, F., Wang, J., Kelly, M., 2012. The Holocene Indian monsoon variability over the southern Tibetan Plateau and its teleconnections. Earth Planet. Sci. Lett. 335–336, 135–144.

Carbonel, P., Colin, J.P., Daneilopol, D.L., Loffler, H., Neustrueva, I., 1988. Paleoecology of limnic ostracodes: A review of some major topics. Palaeogeogr. Palaeoclimatol. Palaeoecol. 62, 413–461.

Chalaturnyk, M.M., Last, W.M., Solylo, P., 2005. Carbonate hardgrounds in maars of western Victoria, Australia; a glimpse at modern lacustrine dolomite formation. In: Annual Meeting, vol. A25. American Association of Petroleum Geologists, p. 14.

Cheng, H., Fleitmann, D., Edwards, L.R., Wang, X., Cruz, F.W., Auler, A.S., Mangini, A., Wang, Y., Kong, X., Burns, S.J., Matter, A., 2009. Timing and structure of the 8.2 kyr B.P. event inferred from δ^{18}O records of stalagmites from China, Oman and Brazil. Geology 37, 1007–1010.

Chopra, S., 1990. A geological cum geomorphological framework of Haryana and adjoining areas for landuse appraisal using LANDSAT imagery. J. Indian Soc. Remote Sensing 1–2, 15–22.

Craig, H., Gordon, L.I., 1965. Deuterium and oxygen-18 variations in the ocean and the marine atmosphere. In: Stable Isotopes in Oceanographic Studies and Paleotemperatures. Pisa, pp. 9–130.

Durazzi, J.T., 1977. Stable isotopes in ostracod shells – preliminary-study. Geochim. Cosmochim. Acta 41, 1168–1170.

Engleman, E.E., Jackson, L.L., Norton, D.R., 1985. Determination of carbonate carbon in geological materials by coulometric titration. Chem. Geol. 53, 125–128.

Enzel, Y., Ely, L.L., Mishra, S., Ramesh, R., Amit, R., Lazar, B., Rajaguru, S.N., Baker, V.R., Sandler, A., 1999. High-resolution Holocene environmental changes in the Thar Desert, northwestern India. Science 284, 125–128.

Fasullo, J., Webster, P.J., 2003. A hydrological definition of Indian monsoon onset and withdrawal. J. Climate 16, 3200–3211.

Fleitmann, D., Burns, S.J., Mudelsee, M., Neff, U., Kramers, J., Mangini, A., Matter, A., 2003. Holocene forcing of the Indian monsoon recorded in a stalagmite from Southern Oman. Science 300, 1737–1739.

Fleitmann, D., Burns, S.J., Mangini, A., Mudelsee, M., Kramers, J., Villa, I., Neff, U., Al-Subbary, A.A., Buettner, A., Hippler, D., Matter, A., 2007. Holocene ITCZ and Indian monsoon dynamics recorded in stalagmites from Oman and Yemen (Socotra). Quat. Sci. Rev. 26, 170–188.

Govil, P., Naidu, P.D., 2010. Evaporation–precipitation changes in the eastern Arabian Sea for the last 68 ka: Implications on monsoon variability. Paleoceanography 25, PA1210. http://dx.doi.org/10.1029/2008PA001687.

Govil, P., Naidu, P.D., Kuhnert, H., 2011. Variations of Indian monsoon precipitation during the last 32 kyr reflected in the surface hydrography of the western Bay of Bengal. Quat. Sci. Rev. 30, 3871–3879.

Gupta, A.K., Anderson, D.M., Overpeck, J.T., 2003. Abrupt changes in the Asian southwest monsoon during the Holocene and their links to the North Atlantic Ocean. Nature 421, 354–357.

Gupta, A.K., Das, M., Anderson, D.M., 2005. Solar influence on the Indian summer monsoon during the Holocene. Geophys. Res. Lett. 32, L17703.

Heip, C., 1976. Spatial pattern of *Cyprideis torosa* (Jones, 1850) (Crustacea: Ostracoda). J. Mar. Biol. Assoc. UK 56, 179–189.

Herman, P.M.J., Heip, C., Vranken, G., 1983. The production of *Cyprideis torosa* Jones 1850 (Crustacea, Ostracoda). Oecologia 58, 326–331.

Hodell, D.A., Schelske, C.L., Fahnenstiel, G.L., Robbins, L.L., 1998. Biologically induced calcite and its isotopic composition in Lake Ontario. Limnol. Oceanogr. 43, 187–199.

Hodell, D.A., Brenner, M., Kanfoush, S.L., Curtis, J.H., Stoner, J.S., Song, X., Wu, Y., Whitmore, T.J., 1999. Paleoclimate of Southwestern China for the past 50,000 yr inferred from Lake Sediment Records. Quat. Res. 52, 369–380.

Indian Meteorological Department, 2000. Climatological tables of observatories in India (1901–2000), New Delhi. http://www.imd.gov.in/doc/climateimp.pdf.

Jin, Z., Yu, J., Chen, H., Wu, Y., Wang, S., Chen, S., 2007. The influence and chronological uncertainties of the 8.2 ka cooling event on continental climate records in China. Holocene 17, 1041–1050.

Kleiven, H.F., Kissel, C., Laj, C., Ninnemann, U.S., Richter, T.O., Cortijo, E., 2008. Reduced North Atlantic Deep Water coeval with the glacial Lake Agassiz freshwater outburst. Science 319, 60–64.

Kobashi, T., Severinghaus, J.P., Brook, E.J., Barnola, J.-M., Grachev, A.M., 2007. Precise timing and characterization of abrupt climate change 8200 years ago from air trapped in polar ice. Quat. Sci. Rev. 26, 1212–1222.

Kutzbach, J.E., Street-Perott, F.A., 1985. Milankovitch forcing of fluctuations in the level of tropical lakes from 18 to 0 kyr BP. Nature 317, 130–134.

Last, W., 1992. Petrology of modern carbonate hardgrounds from East Basin Lake, a saline maar lake, southern Australia. Sediment. Geol. 81, 215–229.

LeGrande, A.N., Schimdt, G.A., Shindell, D.T., Field, C.V., Miller, R.L., Koch, D.M., Faluvegi, G., Hoffmann, G., 2006. Consistent simulations of multiple proxy responses to an abrupt climate change event. Proc. Natl. Acad. Sci. USA 103, 837–842.

Leng, M.J., Marshall, J.D., 2004. Palaeoclimate interpretation of stable isotope data from lake sediment archives. Quat. Sci. Rev. 23, 811–831.

Leng, M.J., Lamb, A.L., Lamb, H.F., Telford, R.J., 1999. Palaeoclimatic implications of isotopic data from modern and early Holocene shells of the freshwater snail *Melanoides tuberculata*, from lakes in Ethiopian Rift Valley. J. Paleolimnol. 21, 97–106.

Liu, Y.-H., Henderson, G.M., Hu, C.-Y., Mason, A.J., Charnley, N., Johnson, K.R., Xie, S.-C., 2013. Links between the East Asian monsoon and North Atlantic climate during the 8200 year event. Nat. Geosci. 6, 117–120.

Marco-Barba, J., Ito, E., Carbonell, F., Mesquita-Joanes, F., 2012. Empirical calibration of shell chemistry of *Cyprideis torosa* (Jones, 1850) (Crustacea: Ostracoda). Geochim. Cosmochim. Acta 93, 143–163.

Marzin, C., Braconnot, P., 2009. Variations of Indian and African monsoons induced by insolation changes at 6 and 9.5 kyr BP. Clim. Dyn. 33, 215–231.

Morril, C., Anderson, D.M., Bauer, B.A., Buckner, R., Gille, E.P., Gross, W.S., Hartman, M., Shah, A., 2013. Proxy benchmarks for intercomparison of 8.2 ka simulations. Clim. Past 9, 423–432.

Neff, U., Burns, S.J., Mangini, A., Mudelsee, M., Fleitmann, D., Matter, A., 2001. Strong coherence between solar variability and the monsoon in Oman between 9 and 6 kyr ago. Nature 411, 290–293.

Overpeck, J., Anderson, D., Trumbore, S., Prell, W., 1996. The southwest Indian Monsoon over the last 18 000 years. Clim. Dyn. 12, 213–225.

Pausata, F.S.R., Battisti, D.S., Nisancioglu, K.H., Bitz, C., 2011. Chinese stalagmite δ^{18}O controlled by changes in the Indian monsoon during a simulated Heinrich event. Nat. Geosci. 4, 474–480.

Prasad, S., Enzel, Y., 2006. Holocene paleoclimates of India. Quat. Res. 66, 442–453.

Porter, S., An, Z., 1995. Correlation between climate events in the North Atlantic and China during the last glaciation. Nature 375, 305–308.

Rashid, H., Flower, B.P., Poore, R.Z., Quinn, T.M., 2007. A 25 ka Indian Ocean monsoon variability record from the Andaman Sea. Quat. Sci. Rev. 26, 2586–2597.

Rashid, H., England, E., Thompson, L., Polyak, L., 2011. Late glacial to Holocene Indian summer monsoon variability based upon sediment. Terr. Atmos. Ocean. Sci. 22, 215–228.

Rasmussen, S.O., Andersen, K.K., Svensson, A.M., Steffensen, J.P., Vinther, B.M., Clausen, H.B., Siggaard-Andersen, M.L., Johnsen, S.J., Larsen, L.B., Dahl-Jensen, D., Bigler, M., Röthlisberger, R., Fischer, H., Goto-Azuma, K., Hansson, M.E., Ruth, U., 2006. A new Greenland ice core chronology for the last glacial termination. J. Geophys. Res. 111, D06102.

Reimer, P.J., Bard, E., Bayliss, A., Beck, J.W., Blackwell, P.G., Bronk Ramsey, C., Buck, C.E., Burr, G.S., Edwards, R.L., Friedrich, M., Grootes, P.M., Guilderson, T.P., Hajdas, I., Heaton, T.J., Hogg, A.G., Hughen, K.A., Kaiser, K.F., Kromer, B., McCormac, F.G., Manning, S.W., Reimer, R.W., Richards, D.A., Southon, J.R., Talamo, S., Turney, C.S.M., van der Plicht, J., Weyhenmeyer, C.E., 2009. IntCal09 and Marine09 radiocarbon age calibration curves, 0–50 000 years cal BP. Radiocarbon 51, 1111–1150.

Rozanski, K., Araguas-Araguas, L., Gonfiantini, R., 1993. Isotopic patterns in modern global precipitation. In: Swart, P.K., Lohmann, K.C., McKenzie, J., Savin, S. (Eds.), Climate Change in Continental Isotopic Records. American Geophysical Union, Washington, DC, pp. 1–36.

Saini, H.S., Tandon, S.K., Mujtaba, S.A.I., Pant, N.C., 2005. Lake deposits of the northeastern margin of Thar Desert: Holocene(?) Palaeoclimatic implications. Curr. Sci. India 88, 1994–2000.

Sarkar, A., Ramesh, R., Somayajulu, B.L.K., Agnihotri, R., Jull, A.J.T., Burr, G.S., 2000. High resolution Holocene monsoon record from the eastern Arabian Sea. Earth Planet. Sci. Lett. 177, 209–218.

Schulz, H., von Rad, U., Erlenkeuser, H., 1998. Correlation between Arabian Sea and Greenland climate oscillations of the past 110 000 years. Nature 393, 54–57.

Sengupta, S., Sarkar, A., 2006. Stable isotope evidence of dual (Arabian Sea and Bay of Bengal) vapor sources in monsoonal precipitation over north India. Earth Planet. Sci. Lett. 250, 511–521.

Shanahan, T.M., Pigati, J.S., Dettman, D.L., Quade, J., 2005. Isotopic variability in the aragonite shell of freshwater gastropods living in springs with nearly constant temperature and isotopic composition. Geochim. Cosmochim. Acta 69, 3949–3966.

Singh, G., Wasson, R.J., Agrawal, D.P., 1990. Vegetational and seasonal climatic changes since the last full glacial in the Thar Desert, north-west India. Rev. Palaeobot. Palynol. 64, 351–358.

Sinha, A., Cannariato, K.G., Stott, L.D., Li, H., You, C., Cheng, H., Edwards, L.R., Singh, I.B., 2005. Variability of Southwest Indian summer monsoon precipitation during the Bølling–Ållerød. Geology 33, 813–818.

Sinha, R., Smykatz-Kloss, W., Stueben, D., Harrison, S.P., Berner, Z., Kramar, U., 2006. Late Quaternary palaeoclimatic reconstruction from the lacustrine sediments of the Sambhar playa core, Thar Desert margin, India. Palaeogeogr. Palaeoclimatol. Palaeoecol. 233 (3–4), 252–270.

Sirocko, F., Garbe-Schösnberg, D., Mclntyre, A., Molfino, B., 1996. Teleconnections between the subtropical monsoons and high-latitude climates during the last deglaciation. Science 272, 526–529.

Staubwasser, M., Sirocko, F., Grootes, P.M., Erlenkeuser, H., 2002. South Asian monsoon climate change and radiocarbon in the Arabian Sea during early and middle Holocene. Paleoceanography 17 (4), 1063. http://dx.doi.org/10.1029/2000PA000608.

Staubwasser, M., Sirocko, F., Grootes, P.M., Segl, M., 2003. Climate change at the 4.2 ka BP termination of the Indus valley civilization and Holocene south Asian monsoon variability. Geophys. Res. Lett. 30, 1425. http://dx.doi.org/10.1029/2002GL016822.

Talbot, M.R., 1990. A review of the palaeohydrological interpretation of carbon and oxygen isotopic-ratios in primary lacustrine carbonates. Chem. Geol. 80, 261–279.

Thomas, E.R., Wolff, E.W., Mulvaney, R., Steffensen, J.P., Johnsen, S.J., Arrowsmith, C., White, J.W.C., Vaughn, B., Popp, T., 2007. The 8.2 ka event from Greenland ice cores. Quat. Sci. Rev. 26, 70–81.

Wang, Y., Cheng, H., Edwards, R.L., An, Z.S., Wu, J.Y., Shen, C.C., Dorale, J.A., 2001. A high-resolution absolute-dated Late Pleistocene monsoon record from Hulu Cave, China. Science 294, 2345–2348.

Wang, Y., Cheng, H., Edwards, R.L., He, Y., Kong, X., An, Z., Wu, J., Kelly, M.J., Dykoski, C.A., Li, X., 2005. The Holocene Asian monsoon: Links to solar changes and North Atlantic climate. Science 308, 854–857.

Zhang, J.W., Chen, F.H., Holmes, J.A., Li, H., Guo, X.Y., Wang, J.L., Li, S., Lu, Y.B., Zhao, Y., Qiang, M.R., 2011. Holocene monsoon climate documented by oxygen and carbon isotopes from lake sediments and peat bogs in China: a review and synthesis. Quat. Sci. Rev. 30, 1973–1987. http://dx.doi.org/10.1016/j.quascirev.2011.04.023.